Charge Exchange. II. Proton-Hydrogen-Atom Total and Excited-State Cross Sections*†

Yehuda B. Band
Department of Physics, University of Chicago, Chicago, Illinois 60637
(Received 2 April 1973)

By using the method proposed in a previous paper the differential and integrated capture cross sections for the processes $p + H(1s) \rightarrow H(nl) + p$ are computed as a function of incident kinetic energy, for energies of 25 keV and higher, and compared with experiment. The results are compared with the Jackson and Schiff scaling rules and are used to compute the total charge-exchange cross section for proton–hydrogen-atom collisions.

I. INTRODUCTION

In a previous paper[1] (I) we proposed a method of calculating cross sections for rearrangement collisions taking into account the nonorthogonality of initial and final states. We applied the method to proton–hydrogen-atom charge-exchange collisions at incident relative energies above 25 keV. In particular, we calculated the differential and total cross section for $1s \rightarrow 1s$ charge-exchange transitions. The terms in our matrix element which "correct" for the nonorthogonality of initial and final states significantly alter the cross section as calculated using the method of Jackson and Schiff.[2] Since the $1s \rightarrow 1s$ charge-exchange transition cannot be observed directly, assumptions concerning the $1s \rightarrow nl$ cross sections are necessary to compare our results with the experimental data on the total charge-exchange cross sections σ_{total}. We assumed that multiplication of our ground-state cross section $\sigma_{1s \rightarrow 1s}$ by the ratio determined by Jackson and Schiff[2] from the scaling laws postulated in their paper would lead to a reasonable estimate of the total charge-exchange cross section. We found reasonable agreement with the data of McClure,[3] Bayfield,[4] and Gilbody and Ryding[5] above 25 keV, below which the Born approximation fails.

In this paper we shall calculate the charge-exchange cross sections $\sigma_{1s \rightarrow nl}$ into excited states using the formalism proposed in I and a computational method that will allow us to calculate the cross sections into excited states with ease. These cross sections may be directly observed in the laboratory by observing the Doppler-shifted radiation emitted from the decay of the excited states. We shall compare our results with the experiments of Bayfield[4] and Ryding, Wittkower, and Gilbody.[6] The determination of $\sigma_{1S \rightarrow nl}$ will also serve to check the assumptions that went into determining σ_{total} in I.

Previous attempts at including nonorthogonality corrections into the calculation of $p + H$ charge-exchange include the work of Bassel and Gerjouy,[7] Bates,[8] McCarroll,[9] and McElroy.[10] Bassel and Gerjouy[7] use a distorted-wave approximation. Their cross section tends asymptotically to the Brinkman-Kramers[11] result at higher energies and are larger than experimental observations of the total charge-exchange cross section at these energies. Bates[8] uses an impact-parameter formalism with straight line trajectories (so that without further assumptions concerning the legitimacy of extracting a transition matrix element which depends upon the scattering angle, a differential cross section cannot be obtained). McCarroll[9] applied the method of Bates to obtain the $p + H(1s) \rightarrow H(1s) + p$ cross section. Asymptotically, this result also tends to the Brinkman-Kramers cross section. McElroy[10] calculates cross sections for $p + H(1s) \rightarrow H(2s) + p$ and $p + H(1s) \rightarrow H(2p) + p$, using the Bates method. The results again tend to the Brinkman-Kramers cross sections. Measurements of the higher-energy dependence of excited-state charge exchange have not yet been carried out so there is as yet no comparison with experiment at these higher energies and the asymptotic energy dependence of excited state cross sections is an open question. The present method for calculating the charge-exchange processes $p + H(1s) \rightarrow H(nl) + p$ tends asymptotically to the Jackson and Schiff cross sections (with good agreement with experiments on the total charge-exchange cross section). A close-coupling method[12] for calculating proton-hydrogen scattering has been used by Cheshire, Gallaher, and Taylor.[13] They include pseudostates in order to simulate some molecular features at small nuclear separations. An impact-parameter approach with straight-line trajectories is used. Their results are in good agreement with total charge-exchange data. For $\sigma_{1S \rightarrow 2S}$ their calculations are in agreement with the data of Bayfield[4] and Ryding *et al.*[6] except at low energies, below about 6 keV and in the region 15–40 keV. Cheshire *et al.* drop from the Hamiltonian the $1/R$ Coulomb interaction between the protons. If this term were left out of the present method, we would obtain cross sec-

tions not far from the Brinkman-Kramers results. This problem was discussed in some detail previously.[1]

It is useful to review the range of validity of our method. We are concerned with charge-exchange collisions involving A and $(B+e)$ where there is no long-range Coulomb potential between them. A and B should be such that they can be considered as cores with respect to the orbit of the "active" electron. We should be able to ignore all other channels except the elastic channel in determining the charge-exchange cross section into the channel of interest. That is, to a good approximation, all but the elastic channel should decouple from the charge-exchange channel of interest. An order-of-magnitude estimate of the range of the kinetic energy for which our method is expected to work was obtained in I. When A and B are light atoms we find that the method should be valid for relative energies above 10 keV. This condition is satisfied in dealing with the processes $p+\mathrm{H}\rightarrow \mathrm{H}(nl)+p$ with incident proton energies above 25 keV in the laboratory frame, with slow H-atom targets.

II. CALCULATION OF EXCITED FINAL STATES

The transition matrix element for charge-exchange collisions into nlm states from $1s$ states is given by

$$T_{fi}=(h_{fi}-S_{fi}h_{ii})/(1-|S_{fi}|^2),$$

where the final state f is the nlm state of the electron about the incident proton A, the initial state i is the $1s$ state of the electron about the target proton B, S_{fi} is an overlap integral, and the h's are the matrix elements of the potentials responsible for the charge exchange. Explicit expressions for these terms are given in Eqs. (20), (21), and (24) of I.

In order to calculate the terms in the transition matrix element we define, following Sec. III of I, the vectors[14]

$$\vec{B}=\vec{k}_f-\vec{k}_i\left(1-\frac{1}{M_B+1}\right), \tag{1}$$

$$\vec{C}=\vec{k}_f\left(1-\frac{1}{M_A+1}\right)-\vec{k}_i, \tag{2}$$

where $\vec{k}_i$ and $\vec{k}_f$ are the relative momentum of A and $(B+e)$ in the initial state and the relative momentum of $(A+e)$ and B in the final state, respectively. Conservation of energy requires that the energy of the initial and final states be equal, so that for particles of equal mass ($M_A=M_B=M$),

$$k_f^2=k_i^2+\rho, \tag{3}$$

where

$$\rho=M(\beta-\alpha) \tag{4}$$

and β and α are the energies of the electron in the $1s$ and nl states, respectively. Squaring $\vec{B}$ and $\vec{C}$ and expressing the results in terms of the incident proton energy E, and the parameter λ defined by

$$\lambda=4(M+1)^2\sin^2\tfrac{1}{2}\theta, \tag{5}$$

where θ is the c.m. scattering angle, we find to lowest order in m_e/M,

$$B^2=E[(1+\rho/2ME)^2+\lambda], \tag{6}$$

$$C^2=E[(1-\rho/2ME)+\lambda]. \tag{7}$$

We will need expressions for Θ(the angle between $\vec{C}$ and $\vec{k}_i$) and $|\vec{B}-\vec{C}|^2$. We obtain

$$\cos\Theta=-\frac{E^{1/2}(1-\rho/2ME)}{C}, \tag{8}$$

$$|\vec{B}-\vec{C}|^2=\frac{1}{(M+1)^2}(\vec{k}_f+\vec{k}_i)^2=4E. \tag{9}$$

From the expression for $|\vec{B}-\vec{C}|^2$ we conclude that

$$\cos(B,C)=(B^2+C^2-4E)/2BC. \tag{10}$$

When the final state is the $1s$ state, these expressions reduce to the expressions obtained in I. Also, the azimuthal angle of $\vec{C}$ when $\vec{k}_i$ defines the z axis and the x axis is arbitrarily chosen will be called Φ.

The transition matrix element for charge-exchange collisons $1s\rightarrow nlm$ can now be written as

$$T_{nlm}(E,\lambda,\Phi)=\frac{a(n,c^2)\varphi^*_{nlm}(\vec{C})\varphi_{100}(\vec{B})+(1/2\pi^2)\int(d^3k/k^2)\varphi^*_{nlm}(\vec{C}-\vec{k})\varphi_{100}(\vec{B}-\vec{k})}{(2\pi)^3[1-|\varphi^*_{nlm}(\vec{C})\varphi(\vec{B})/(2\pi)^3|^2]}, \tag{12}$$

where

$$a(n,C^2)=-\tfrac{1}{2}(C^2+1/n^2+1/2\pi^2) \tag{13}$$

and $\varphi(\vec{p})$ is the wave function in the momentum representation. The integral over $\vec{k}$ represents the contribution to the transition matrix element due to the proton-proton potential.

For ground-state charge exchange the simple forms of the wave functions allow us to evaluate the integral over $\vec{k}$ analytically (up to one quadrature) using an auxiliary-integral technique.[1,7,15,16] For excited states it is possible to express the integral over $\vec{k}$ as a linear combination of terms involving derivatives of an auxiliary integral with respect to a parameter a and the components of $\vec{C}$ [see Eqs. (49) and (50) of I]. The auxiliary integral

is then numerically integrated. Such a technique quickly becomes unmanageable for higher excited states, especially when the correction terms are included. We choose a different technique which can be programmed without taking any complicated derivatives and whose algorithm need not be changed if we wish to change Z_A or Z_B, or even change the wave function.

Let $\mathcal{R}$ denote a rotation of the coordinate system which takes $\vec{C} \to \vec{C}'$ and $\vec{B} \to \vec{B}'$ where $\vec{C}'$ is along the $-z$ axis and $\vec{B}'$ in the $x-z$ plane (see Fig. 1). Then we can express $T_{nlm}(E, \lambda, \Phi)$ as

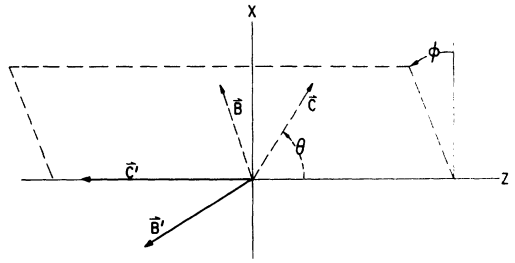

FIG. 1. Vectors $\vec{B}$, $\vec{C}$, $\vec{B}'$, and $\vec{C}'$. $\vec{B}$ and $\vec{C}$ lie in a plane which makes an angle Φ with the x-z plane. $\vec{B}'$ and $\vec{C}'$ lie in the x-z plane.

$$T_{nlm}(E,\lambda,\Phi)=\frac{D^{[l]}_{\mu m}(\mathcal{R})[a(n,C^2)\varphi^*_{nl\mu}(\vec{C}')\varphi_{100}(\vec{B}')+(1/2\pi^2)\int(d^3k'/k'^2)\varphi^*_{nl\mu}(\vec{C}'-\vec{k}')\varphi_{100}(\vec{B}'-\vec{k}')]}{(2\pi)^3[1-|\varphi_{nlm}(\vec{C})\varphi_{100}(\vec{B})/(2\pi)^3|^2]}\,, \tag{14}$$

where[17]

$$D^{[l]}_{\mu m}(\mathcal{R})=\langle l\mu\,|\mathcal{R}|\,lm\rangle = d^l_{\mu m}(-(\pi-\theta))\,e^{-im\Phi} \tag{15}$$

and the sum over μ is implied. From expression (14) we can see that $|T_{nlm}(E,\lambda,\Phi)|^2$ is independent of Φ, which means the cross section has cylindrical symmetry. The integral over $\vec{k}'$ may now be evaluated. Let x be the cosine of the angle between $\vec{k}'$ and $\hat{z}$ and φ be the azimuthal angle of $\vec{k}'$. Then we find

$$|\vec{C}'-\vec{k}'|=C^2+k^2+2Ckx\,, \tag{16}$$

$$\cos(\vec{C}'-\vec{k}',\hat{z})=\frac{-(C+kx)}{(C^2+k^2+2Ckx)^{1/2}}\,, \tag{17}$$

$$|\vec{B}'-\vec{k}'|=B^2+k^2-2Bk[x(-1)\cos(B,C)+\cos\varphi\,\sin(B,C)(1-x^2)^{1/2}]\,. \tag{18}$$

With the expressions for $\varphi(\vec{p})$, the integral over $\vec{k}'$ may be reduced to a two-dimensional integral by working out the integral over φ (see Appendix). The two-dimensional integral is computed numerically. The final result for the matrix element T_{nlm} is

$$T_{nlm}(E,\lambda,\Phi)=\left(\frac{1}{1-N_{nl}f^2_{nl}(C)f^2_{10}(B)\theta^2_{lm}(\cos\Theta)/2\pi}\right)\left(\frac{N_{nl}}{2\pi}\right)^{1/2}d^{[l]}_{\mu m}(-\Theta)e^{-im\Phi}$$
$$\times\Bigg[a(n,C^2)f_{nl}(C)\theta_{l\mu}(-1)f_{10}(B)+\frac{(-1)^{l+m}}{\pi}\int_0^\infty dk\int_{-1}^1 dx f_{nl}((C^2+k^2+2Ckx)^{1/2})\theta_{l\mu}\left(\frac{C+kx}{(C^2+k^2+2Ckx)^{1/2}}\right)$$
$$\times\frac{1}{a^2-b^2}\left(m+\frac{a}{(a^2-b^2)^{1/2}}\right)\left(\frac{-a+(a^2-b^2)^{1/2}}{b}\right)^{|m|}\Bigg]\,, \tag{19}$$

where $\Theta_{lm}(\cos\theta)$ is defined by the equation

$$Y_{lm}(\Omega)=[e^{im\varphi}/(2\pi)^{1/2}]\Theta_{lm}(\cos\theta) \tag{20}$$

and

$$a=1+B^2+k^2+2Bkx\cos(B,C)\,, \tag{21}$$

$$b=2Bk\sin(B,C)(1-x^2)^{1/2}\,, \tag{22}$$

$$N_{nl}=\left(\frac{16n^2 4^l l!}{\pi^{3/2}}\right)^2\frac{(n-l-1)!}{(n+l)!} \tag{23}$$

$$f_{nl}(x)=(nx)^l C^{l+1}_{n-l-1}\left(\frac{(nx)^2-1}{(nx)^2+1}\right)\Big/[(nx)^2+1]^{l+2}\,, \tag{24}$$

and $C^\alpha_\beta(x)$ is the Gegenbauer polynomial.

The differential cross section for $1s \to nl$ transitions

$$\frac{d\sigma_{1s\to nl}}{d\Omega}=(2\pi)^4\frac{k_f}{k_i}\left(\frac{M}{2}\right)^2\sum_{m=-l}^{l}|T_{nlm}|^2 \tag{25}$$

may now be computed using Eq. (19) for $T_{nlm}(E, \lambda, \Phi)$. By calling the first factor unity in Eq. (19), and neglecting the last term in Eq. (13) for $a(n, C^2)$, we obtain the Jackson and Schiff matrix element. When these approximations are made, a simplification for the cross section results be-

cause the D functions satisfy

$$\sum_{m=-l}^{l} D^{[l]}_{\mu m}(R) D^{*[l]}_{\nu m}(R) = \delta_{\mu\nu} . \tag{26}$$

Note that if the first term in Eq. (19) is not approximated by 1, then we cannot use Eq. (26) because the first term of (19) is a function of m and the sum over m is weighted in (26). The total cross section is obtained by integrating the differential cross section:

$$\sigma_{1s\to nl} = \frac{2\pi}{2M^2} \int d\lambda \frac{d\sigma_{1s\to nl}}{d\Omega} .$$

III. DISCUSSION OF RESULTS

A. Differential Cross Sections

The angular distributions for charge-exchange collisions into various states as given by the present calculation (which include the nonorthogonality corrections) are shown in Figs. 2 and 3. For charge exchange into the $2s$ state a dip appears in the angular distribution, similar to the dip in the $1s$ angular distribution.[18] The origin of this dip seems to be the cancellation of the terms in the transition matrix element due to the electron-proton and proton-proton potentials. In the forward peak the electron-proton term dominates the matrix element and at the larger angles, beyond the dip, the proton-proton term dominates and gives rise to the tail of the distribution. This may be understood by noting that the smaller angles correspond to large impact parameters where the electron-proton potential dominates. Most of the cross section comes from the small-angle scattering region. There is considerable structure in the angular distribution at angles greater than the "dark angle." The $2p$ angular distribution has a shallow minimum but nothing like the "dark angle" in the $1s$, $2s$, or higher ns differential cross sections.

The $2s$ and $2p$ differential cross sections are of comparable magnitude, which is the reason for the scaling of the $2p$ in Fig. 2. The very steep slope in the extreme forward direction and then the more gradual decrease of the angular distribution with larger angles is a feature present in all the angular distributions plotted. The cross sections for s and p charge exchange are considerably larger than the cross sections for final states of higher angular momentum. All of the distributions decrease in magnitude with increasing E at any given value of λ.

All of the differential cross sections for charge exchange into ns states have a "dark angle" the origin of which has already been mentioned. As the incident proton energy is increased, the dark angle moves to smaller θ and the width of the dark zone decreases. For a fixed energy the position of the dark angle is not sensitive to the principal quantum number of the final excited state. That is, the dark angle for $n=2, 3, 4$, or even 11 ($n=4$, 11, $l=0$, have been calculated but have not been plotted) appear at about the same position at a

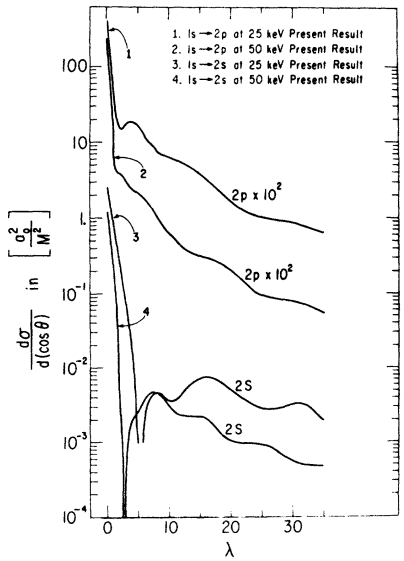

FIG. 2. Differential cross section for charge exchange into the $2s$ and $2p$ states.

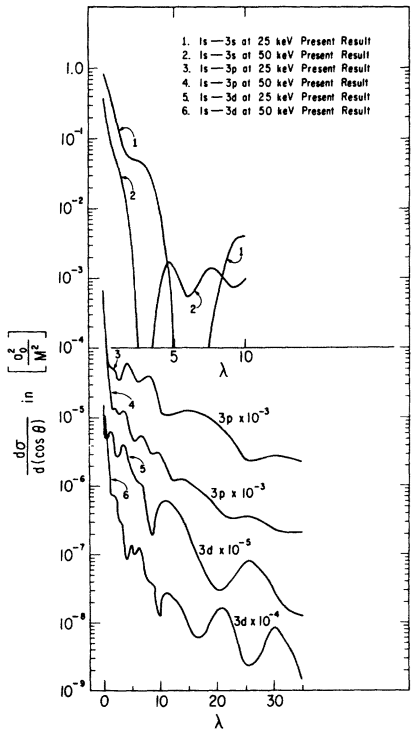

FIG. 3. Differential cross section for charge exchange into $3s$, $3p$, and $3d$ states.

given energy. In Fig. 3 we can see that the 3*s* cross section has an inflection before the dark angle. The 4*s* angular distribution has an even more drastic inflection (actually a shallow minimum for 25 keV) before the dark angle. As the energy is increased the inflections become less pronounced. It is the proton-proton term which is responsible for the inflections as well as the structure in the angular distribution at angles greater then the "dark angle".

B. Possible Observations

All the differential cross sections are extremely forward peaked. The scattering into one-tenth of a degree in the laboratory frame where the incident proton collides with the stationary hydrogen atom corresponds to scattering into the range of $\lambda < 41$ and the structure of the differential cross sections within such small solid angles is difficult to detect. Experiments to measure the differential cross section are feasible, however, by doing the experiment in a frame in which the protons are slow and the hydrogen atoms in the 1*s* state have large kinetic energies, or in a clashing beam geometry. The fast-atom–slow-ion configuration can be accomplished by passing an energetic proton beam (> 25 keV) through a foil to achieve charge exchange, then allowing the beam to traverse a distance long enough for most of the excited states to decay to either the 1*s* or 2*s* state. The beam then passes through a Stark field to quench the metastables, ionize any remaining high Rydberg states, and remove any free protons or electrons and finally into the collision region where it collides with a slow beam of protons. The atoms produced can now be detected over a resolvable range of angles.

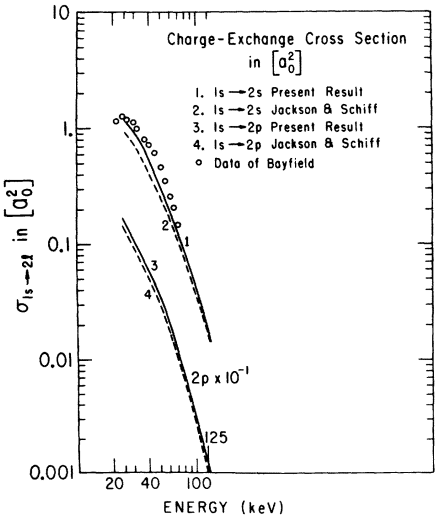

FIG. 4. Cross sections for charge exchange into 2*s* and 2*p*. Data of Bayfield for 2*s* contains contributions from cascade processes.

C. Integrated Cross Sections

Figures 4–6 show integrated charge-exchange cross sections into specified states as a function of incident proton energy. "Corrected" and "uncorrected" Born approximation cross sections are indicated by solid and broken lines, respectively; "corrected" means that the nonorthogonality terms are retained. The cross sections are tabulated in Table I. Our calculation using the Jackson and Schiff matrix element agrees with that of Mapleton[19] for the energies and states for which our calculations overlap. Figures 7–9 indicate the ratio of the difference between corrected and uncorrected cross sections to the uncorrected cross section as a function of energy. The nonorthogonality corrections become less important as the energy increases for each of the final-state cross sections and as the angular momentum number of the final state increases.

Figure 4 plots the data of Bayfield[4] in the energy range where our method is valid. The data of Ryding, Wittkower, and Gilbody[6] have not been plotted because theirs is a relative, not an absolute cross-section measurement. If their data is

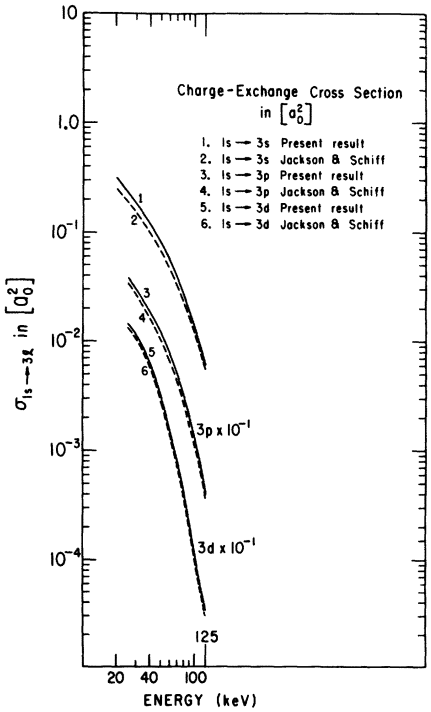

FIG. 5. Cross sections for charge exchange into 3*s*, 3*p*, and 3*d*.

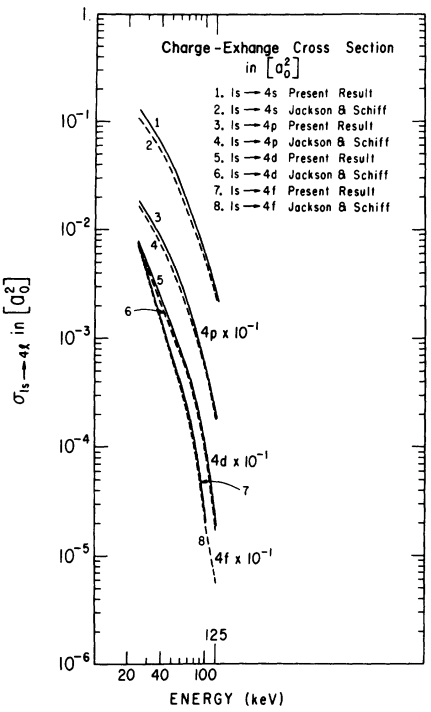

FIG. 6. Cross sections for charge exchange into $4s$, $4p$, $4d$, and $4f$.

normalized to our calculation at 43 keV, then the data are in agreement with the solid curve corresponding to the nonorthogonality-corrected calculation to within the uncertainty in the relative cross section claimed by Ryding *et al.* The correction terms raise the $2s$ cross section substantially above the Jackson and Schiff Born approximation, bringing the theoretical predictions up much closer to the experimental results.

The agreement with experiment is even better than is indicated by the correction terms alone. We note that the experiment measures the Ly-α

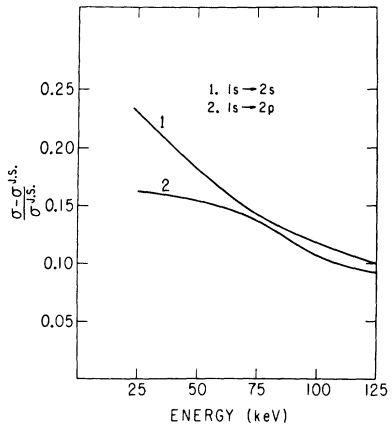

FIG. 7. $(\sigma-\sigma^{JS})/\sigma^{JS}$ for $2s$ and $2p$ cross sections. Jackson and Schiff are abbreviated JS.

TABLE I. Charge-Exchange cross sections (in units of a_0^2).

	Correction terms included					Uncorrected Born Approximation				
Energy (keV)	25	50	75	100	125	25	50	75	100	125
$1s$	9.279	1.891	0.6201	0.2527	0.1178	7.222	1.635	0.5503	0.2308	0.1131
$2s$	1.143	0.2974	0.1021	4.133×10^{-2}	1.896×10^{-2}	0.9288	0.2516	8.929×10^{-2}	3.697×10^{-2}	1.723×10^{-2}
$2p$	1.684	0.3798	0.1006	3.263×10^{-2}	1.260×10^{-2}	1.448	0.3291	8.930×10^{-2}	2.948×10^{-2}	1.155×10^{-2}
$3s$	0.3080	8.191×10^{-2}	3.113×10^{-2}	1.342×10^{-2}	6.039×10^{-3}	0.2515	6.846×10^{-2}	2.707×10^{-2}	1.197×10^{-2}	5.474×10^{-3}
$3p$	0.3856	0.1192	3.866×10^{-2}	1.229×10^{-2}	4.410×10^{-3}	0.3458	0.1033	3.433×10^{-2}	1.110×10^{-2}	4.028×10^{-3}
$3d$	0.1448	3.117×10^{-2}	5.930×10^{-3}	1.090×10^{-3}	3.353×10^{-4}	0.1351	2.791×10^{-2}	5.393×10^{-3}	9.955×10^{-4}	3.087×10^{-4}
$4s$	0.1298	3.805×10^{-2}	1.282×10^{-2}	5.684×10^{-3}	2.659×10^{-3}	0.1066	3.203×10^{-2}	1.110×10^{-2}	5.064×10^{-3}	2.411×10^{-3}
$4p$	0.1829	5.061×10^{-2}	1.554×10^{-2}	5.797×10^{-3}	2.085×10^{-3}	0.1627	4.382×10^{-2}	1.374×10^{-2}	5.237×10^{-3}	1.905×10^{-3}
$4d$	7.434×10^{-2}	1.225×10^{-2}	3.922×10^{-3}	9.417×10^{-4}	2.053×10^{-4}	7.238×10^{-2}	1.119×10^{-2}	3.573×10^{-3}	8.675×10^{-4}	1.900×10^{-4}
$4f$	6.743×10^{-2}	6.990×10^{-3}	1.474×10^{-3}	2.114×10^{-4}	5.996×10^{-5}	6.816×10^{-2}	6.857×10^{-3}	1.437×10^{-3}	2.100×10^{-4}	6.015×10^{-5}
Total of excited states	4.120	1.017	0.3122	0.1134	4.735×10^{-2}	3.519	0.8744	0.2752	0.1109	4.594×10^{-2}
Total	13.399	2.909	0.9323	0.3661	0.1652	10.740	2.509	0.8255	0.3417	0.1590
$2s$ corrected	1.237	0.3248	0.1294	4.443×10^{-2}	2.014×10^{-2}	1.011	0.2753	9.706×10^{-2}	3.974×10^{-2}	1.830×10^{-2}
$\frac{\sigma^{total}-\sigma^{total}_{JS}}{\sigma^{total}_{JS}}$	0.248	0.159	0.129	0.071	0.039					

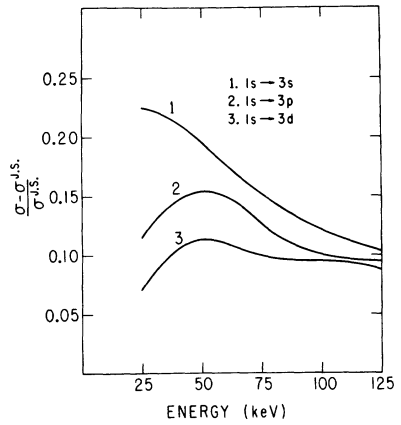

FIG. 8. $(\sigma-\sigma^{JS})/\sigma^{JS}$ for $3s$, $3p$, and $3d$ cross sections.

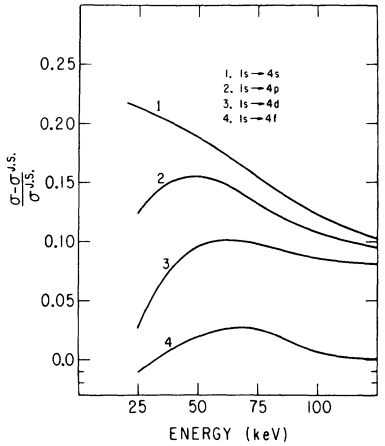

FIG. 9. $(\sigma-\sigma^{JS})/\sigma^{JS}$ for $4s$, $4p$, $4d$, and $4f$ cross sections.

radiation resulting from Stark quenching, so that the observed Ly-α radiation contains contributions from cascades out of higher states, as well as from direct capture into the 2S level. This cascade effect can be taken into account by multiplying the charge-exchange cross section by the branching ratio from the higher excited states to decay into the $2s$ state. We denote this additional $2s$ contribution by R and define Δ to equal $R/\sigma(2S)$ and $P(a\rightarrow b)/\sum P(a)$ to be the probability of state a decaying to state b. Table II indicates the formula for R and tabulates Δ as a function of energy for the corrected calculation and the Jackson and Schiff calculation. Figure 10 shows the cross section $1s\rightarrow 2s$ including cascade from higher states,

$$\sigma_{1s\rightarrow 2s}=\sigma(2s)(1+\Delta).$$

It is interesting to take the ratio

$$\sum_{l=0}^{n-1}\sigma(nl)/\sum_{l=0}^{1}\sigma(2l)$$

so that a comparison can be made with the postulate of Jackson and Schiff that this ratio should be $(2/n)^3$ regardless of the energy of the incident proton. Values are given in Table III and the results are plotted in Fig. 11.

The total charge-exchange cross sections into all states (through $n=4$) are given in Table I and Fig. 12. The agreement between the present theory and the experiments of Bayfield,[4] McClure,[3] and Gilbody and Ryding[5] is good. Including states of $n>5$ will not raise the total cross section substantially. The agreement between theory and experiment is better here than when the Jackson and Schiff scaling laws are used to take the excited states into account.[20]

IV. CONCLUSION AND REMARKS

Agreement between the present theory and the experiments on total charge exchange and charge exchange into the $2s$ state is very satisfactory. The orthogonality corrections and the calculations

TABLE II. $\Delta\equiv R/\sigma(2s)$ as a function of E (in units of keV), where

$$R=\left(\sigma(3p)+\sigma(4s)\frac{P(4s\rightarrow 3p)}{\sum P(4s)}+\sigma(4d)\frac{P(4d\rightarrow 3p)}{\sum P(4d)}+\sigma(5s)\frac{P(5s\rightarrow 3p)}{\sum P(5s)}\right)\frac{P(3p\rightarrow 2s)}{\sum P(3p)}$$
$$+\left(\sigma(5s)\frac{P(5s\rightarrow 4p)}{\sum P(5s)}+\sigma(4p)\right)\frac{P(4p\rightarrow 2s)}{\sum P(4p)}+\sigma(5p)\frac{P(5p\rightarrow 2s)}{\sum P(5p)}.$$

	Energy (keV)				
	25	50	75	100	125
Present calculation	0.082	0.092	0.086	0.075	0.062
Jackson and Schiff	0.089	0.094	0.087	0.075	0.062

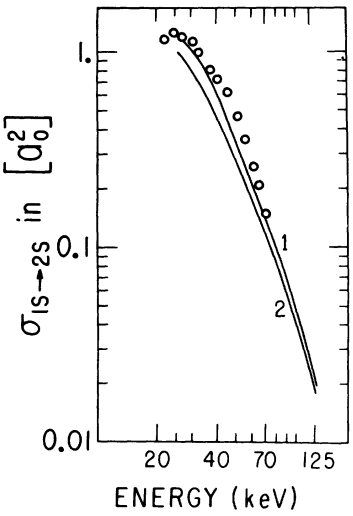

FIG. 10. Charge-exchange cross section $1s \to 2s$ including cascade from higher states. Curve 1: present result; curve 2: using the Jackson and Schiff matrix element; ○: data of Bayfield.

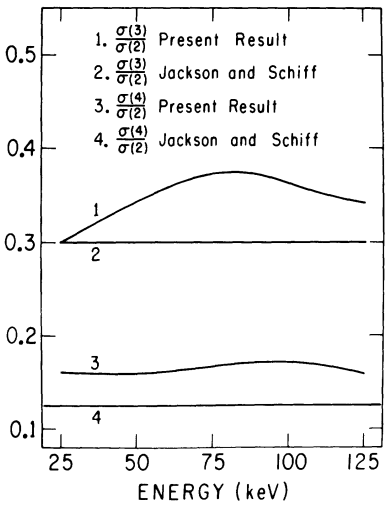

FIG. 11. $\sigma(3)/\sigma(2)$ and $\sigma(4)/\sigma(2)$. Jackson and Schiff scaling rules compared with the results of the present calculation.

for capture into excited states yield results for the total charge-exchange cross section which lie on the data points for incident proton energies of 25 keV and above. The calculations of Bassel and Gerjouy and the calculations based upon the Bates method performed by McCarroll and McElroy are higher than the experimental data above 100 keV.[21] The results of the calculation of Cheshire *et al.* are a little below the total charge-exchange data but are in good agreement with it. For capture into the 2*s* state we obtain good agreement with the data of Bayfield[4] which are absolute cross-section measurements, and with the data of Ryding, Wittkower, and Gilbody[6] when their relative cross-section data is normalized to our result at 43 keV, as mentioned in the previous section. The calculations of Cheshire *et al.* for capture into the 2*s* state are in better agreement with the data of Ryding *et al.* if Ryding's original normalization is used. Measurements of σ_{2s} at higher energies are still necessary to determine the correct asymtotic energy dependence. Experiments to determine σ_{2p} above 25 keV are also called for. To test the theory properly, differential cross-section measurements are crucial.

With the very real possibility of the construction of a 100-keV proton scanning microscope[22] capable of reaching resolution in the 1-Å region and using charge-transfer processes to provide a component of the information that is used in the assembly of the "picture" of the specimen, the theory of charge-transfer processes in this energy range takes on new importance. Before charge transfer from molecules with complex structures can be understood we must be able to understand the theory of the simplest charge-transfer processes. It is hoped that this presentation has helped in some measure to the understanding of simple charge transfer.

We are presently applying the method proposed in I to calculate the charge exchange into high Rydberg states in an attempt to explain the data of Barnett, Ray, and Russek.[23] We shall also apply the method to calculate the ionization cross section in the forward peak measured by Rudd, Sautter, and Baily.[24]

TABLE III. Ratio of cross sections $\sum_l \sigma(nl)/\sum_{l=0}^{1}\sigma(2l)$.

	Correction terms included					Uncorrected Born approximation					Postulated Jackson and Schiff scaling rules
Energy (keV)	25	50	75	100	125	25	50	75	100	125	
$\sigma(3)/\sigma(2)$	0.297	0.343	0.374	0.362	0.342	0.308	0.344	0.374	0.362	0.340	0.296
$\sigma(4)/\sigma(2)$	0.161	0.159	0.166	0.171	0.159	0.172	0.162	0.167	0.171	0.159	0.125

ACKNOWLEDGMENTS

The author is grateful to Professor R. S. Berry for his advice, encouragement and many helpful suggestions throughout the course of this research.

APPENDIX

The integral over $\vec{k}'$ may be written in terms variables defined in Eqs. (20)–(24) of the text as

$$\int \frac{d^3k'}{k'^2}\varphi^*_{nlm}(\vec{C}'-\vec{k}')\varphi_{100}(\vec{B}'-\vec{k}')$$

$$=\left(\frac{N_{nl}}{2\pi}\right)^{1/2}\int\frac{d^3k'}{k'^2}f_{nl}(|\vec{C}'-\vec{k}'|)$$

$$\times\theta_{lm}(\cos(\vec{C}'-\vec{k}',\hat{z}))e^{im\varphi}f_{10}(|\vec{B}'-\vec{k}'|). \quad \text{(A1)}$$

using Eqs. (18) and the form of $f_{10}(x)$,

$$f_{10}(x)=1/(x^2+1)^2,$$

we obtain for the right-hand side of (A1)

$$(-1)^{l+m}\left(\frac{N_{nl}}{2\pi}\right)^{1/2}\int dk'\int_{-1}^{1}dx f_{nl}((C^2+k^2+2Ckx)^{1/2})\theta_{lm}\left(\frac{C+kx}{(C^2+k^2+2Ckx)^{1/2}}\right)$$

$$\times\int_0^{2\pi}d\varphi\, e^{im\varphi}\frac{1}{\{1+B^2+k^2+2Bkx\cos(B,C)-2Bk\sin(B,C)(1-x^2)^{1/2}\cos\varphi\}^2}. \quad \text{(A2)}$$

The integral over φ is in the form

$$\int_0^{2\pi}d\varphi\frac{e^{im\varphi}}{(a+b\cos\varphi)^2}=-\frac{\partial}{\partial a}\int_0^{2\pi}d\varphi\frac{e^{im\varphi}}{a+b\cos\varphi}, \quad \text{(A3)}$$

where a and b are given in (22) and (23) and $a>|b|>0$. Letting $z=e^{i\varphi}$ and performing the contour integral about a circle of unit radius, we find after some algebra

$$\int_0^{2\pi}d\varphi\frac{e^{im\varphi}}{a+b\cos\varphi}=\frac{2\pi}{(a^2-b^2)^{1/2}}\left(\frac{-a+(a^2-b^2)^{1/2}}{b}\right)^{|m|}. \quad \text{(A4)}$$

Differentiating with respect to a in (A3) and using the result in Eq. (A2) we obtain Eq. (19).

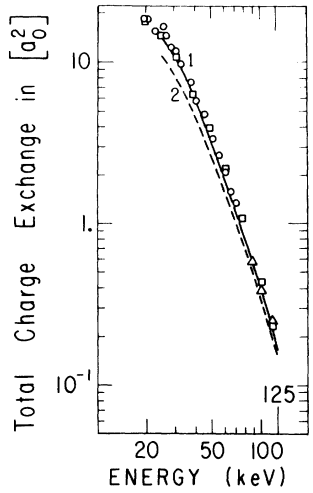

FIG. 12. Total charge-exchange cross section. Curve 1: present result with calculated excited-state charge exchange included; curve 2: Jackson and Schiff with excited-state charge exchange included; ○: data of Bayfield; □: data of McClure; △: data of Gilbody and Ryding.

†This work was supported by the National Science Foundation, Grants GP26493 and 36326X.

*Submitted to the Department of Physics of the University of Chicago in partial fulfillment of the requirements for the degree of Ph.D.

[1]Y. B. Band, Phys. Rev. A 8, 243 (1973), henceforth called I.

[2]J. D. Jackson and H. Schiff, Phys. Rev. 89, 359 (1953).

[3]G. W. McClure, Phys. Rev. 148, 47 (1966).

[4]J. E. Bayfield, Phys. Rev. 182, 115 (1969).

[5]H. B. Gilbody and G. Ryding, Proc. R. Soc. A 291, 438 (1966).

[6]G. Ryding, A. B. Wittkower, and H. B. Gilbody, Proc. Phys. Soc. Lond. 89, 547 (1966).

[7]R. H. Bassel and E. Gerjuoy, Phys. Rev. 117, 749 (1960).

[8]D. R. Bates, Proc. R. Soc. A 247, 294 (1958).

[9]R. McCarroll, Proc. R. Soc. A 264, 547 (1961).

[10]M. B. McElroy, Proc. R. Soc. A 272, 542 (1963).

[11]H. C. Brinkman and H. A. Kramers, Proc. Acad. Sci. Amst. 33, 973 (1930).

[12]L. Wilets and D. F. Gallaher, Phys. Rev. 147, 13 (1966). See also D. F. Gallaher and L. Wilets, Phys. Rev. 169, 139 (1968).

[13]I. M. Cheshire, D. F. Gallaher, and A. J. Taylor, J. Phys. B 3, 813 (1970).

[14]We shall use atomic units throughout.

[15]R. R. Lewis, Phys. Rev. 102, 537 (1956).

[16]R. A. Mapleton, Phys. Rev. 122, 528 (1961).

[17]U. Fano and G. Racah, *Irreducible Tensorial Sets* (Academic, New York, 1959).

[18]See Fig. 2 of Ref. 1.

[19]R. A. Mapleton, Phys. Rev. 126, 1477 (1962).

[20]See Fig. 4 of Ref. 1.

[21]G. Ryding, A. B. Wittkower, and H. B. Gilbody, Proc. Phys. Soc. 89, 541 (1966).

[22]R. Levi Setti, Experimental 100-keV proton Scanning Microscope, National Institute of Health Research Proposal, 1972 (unpublished).

[23]C. F. Barnett, J. A. Ray, and A. Russek, Phys. Rev. A 5, 2110 (1972).

[24]M. E. Rudd, C. A. Sautter, and C. L. Bailey, Phys. Rev. 151, 20 (1966).